EEET ECOLOGICAL ENGINEERING & ENVIRONMENTAL TECHNOLOGY

Ecological Engineering & Environmental Technology 2022, 23(4), 136–148
https://doi.org/10.12912/27197050/150310
ISSN 2719-7050, License CC-BY 4.0

Received: 2022.05.15
Accepted: 2022.05.24
Published: 2022.06.02

The Risk Mapping of Coastal Flooding Areas Due to Tsunami Wave Run-Up Using DAS Model and its Impact on Nekor Bay (Morocco)

Morad Taher[1*], Touafik Mourabit[2], Hajar El Talibi[1], Issam Etebaai[1], Abdelhak Bourjila[3], Ali Errahmouni[2], Mastapha Lamgharbaj[1]

[1] The Department of Earth and Environmental Sciences, The Faculty of Sciences and Technique of Al-Hoceima, The Abdelmalek Essaâdi University, Avenue Khenifra, Tétouan 93000, Morocco

[2] The Department of Geology, The Faculty of Sciences and Techniques of Tanger, The Abdelmalek Essaadi University, Avenue Khenifra, Tétouan 93000, Morocco

[3] Laboratory of Water and Environmental Engineering, Al Hoceima National School of Applied Sciences, The Abdelmalek Essaâdi University, Avenue Khenifra, Tétouan 93000, Morocco

* Corresponing author's e-mail: geomorad@gmail.com

ABSTRACT

The Al-Hoceima region is threatened by tsunami hazard because of its location in the coastal area of the Mediterranean Sea, besides the shallow seismically active region south of the Alboran Sea. Therefore, the current study presents a novel model to map coastal flooding potential zones due to tsunami wave run-up in Nekor bay using three natural parameters (distance from coastline, altitude and slope) in a geographic information system (GIS) environment. Furthermore, the coastal flooding simulation using 4 scénarios (1, 2, 3, 4m) based on the run-up elevation according to tsunami wave elevation (TWE) literature of the study area is used to confirm the DAS model result, and to estimate the potential impacts. The result of the DAS model revealed that 1 km from the coast to the Nekor plain is the most exposed to the impact of tsunamis generated south of the Alboran Sea. The coastal flooding simulation confirmed the DAS result, and the damage estimation of the urban area and the agriculture was respectively 2 and 98% for run-up 1 m, 3% and 97% for run-up 2m, 4% and 96% for run-up 3m, and for the worst case scenario of 4 m was 3% and 97%. Therefore, the results obtained show that the major potential impact of coastal flooding in Nekor plain is the salinization of agricultural land. Finally, we propose a sustainable solution utilizing a controlled forest along the coast to reduce future tsunami impacts on Nekor bay.

Keywords: Al-Hoceima, tsunami hazard, impact, inundation, Nekor.

INTRODUCTION

Coastal flooding or coastal inundation is the product of climate change including Sea Level Rise (SLR) (Amarni et al. 2010; Becu et al. 2017; Bilskie et al. 2014; Cazenave and Cozannet 2014; Ghazali et al. 2018; Al Hatrushi S 2014; Hauer et al. 2021; Jevrejeva et al. 2016; Leatherman, Zhang, and Douglas 2000; Natarajan et al. 2021; Nicholls and Cazenave 2010; Pethick 2001; Qu et al. 2019; Rubinato, Heyworth, and Hart 2020; Samaras and Karambas 2021; Seenath, Wilson, and Miller 2016; Wang and Marsooli 2021; Ward et al. 2011; Werner and Simmons 2009; White, Church, and Gregory 2005) and storm surges (Bilskie et al. 2014; Leatherman, Zhang, and Douglas 2000; Smith et al. 2010), besides tsunami phenomenon (Adrian 2009; J. A. Álvarez-Gómez et al. 2011; José A. Álvarez-Gómez et al. 2011; Amir 2014; Basquin, Mercier, and Creach 2021; Bernard and Titov 2015; Danielsen et al. 2005; Estrada et al. 2021; Fajri et al. 2021; Gonzalez and Medina 1998; Harada and Imamura 2005; Kathiresan and Rajendran 2005; Løvholt et al. 2012; Meyyappan et al. 2015; El Moussaoui et al. 2017; Nandasena, Tanaka, and Tanimoto 2008; Omira et al. 2010; Papadopoulos et al. 2014; Papathoma et al. 2003; Papathoma and Dominey-Howes 2003; Röbke and

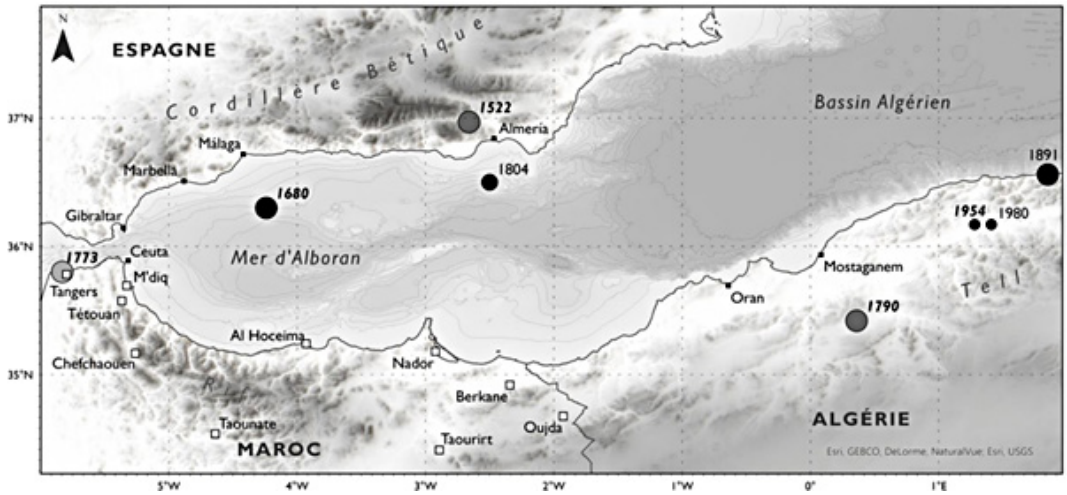

Figure 1. The historical tsunamigenic events in the Alboran Sea (Basquin, Mercier, and Creach 2021)

Vött 2017; Sørensen et al. 2012; Syamsidik et al. 2019; Szczuciński et al. 2006; El Talibi et al. 2016; Vargas et al. 2011; Xie and Chu 2020; Yalciner et al. 2011). Coastal areas all over the world are confronted with serious threats (Ward et al. 2011), because of their ecosystem vulnerability and fragility and their continuous and intense urbanization, mainly in the developing countries (Al Hatrushi S 2014). The Greater national average concentration of infrastructure and economic activities is recently wiedly observed in or around the coastal cities (Jevrejeva et al. 2016; Qu et al. 2019). Therefore, the ecosystems of coastal areas are also threatened by the impact of human activities as well as by natural hazard (Rubinato, Heyworth, and Hart 2020).

Coastal flooding caused massive damages to natural and human resources such as coastal erosion (Al Hatrushi S 2014; Vargas et al. 2011), saltwater intrusion in coastal aquifers (Al Hatrushi S 2014; Nicholls and Cazenave 2010; Werner and Simmons 2009), fisheries, aquaculture, agriculture, tourism, transportation, urbanization also affected by inundation (Al Hatrushi S 2014). The coastal flooding impact increase in low-lying coastal environments and, because of their very low altitude, larger flooded areas and greater impacts were observed in small bays and estuaries (Becu et al. 2017; Bilskie et al. 2014; Röbke and Vött 2017; Samaras and Karambas 2021; Vargas et al. 2011). Therefore, damage estimation is important for the management strategies to protect the coastal areas (Becu et al. 2017; Al Hatrushi S 2014; Samaras and Karambas 2021).

The western Mediterranean has experienced a great development of the tourist and urban sectors during the last decades. The high concentration of population and the significant economic growth that followed in various countries (José A. Álvarez-Gómez et al. 2011) increased considerably the risk of exposure to coastal flooding and tsunami waves (Amir 2014; Danielsen et al. 2005; El Moussaoui et al. 2017; Papadopoulos et al. 2014; Yalciner et al. 2011). Historically, the region has been affected by a significant tsunami generated by the July 21, 365 AD earthquake (Röbke and Vött 2017). More recently, studies of moderate earthquakes such as the 2003 Zemmouri earthquake, show that they can also generate tsunamis (José A. Álvarez-Gómez et al. 2011). The catalog of events counts more than 300 tsunamis (Papadopoulos et al. 2014). Moreover, the Alboran seacoast has witnessed several tsunamis events (Fig.

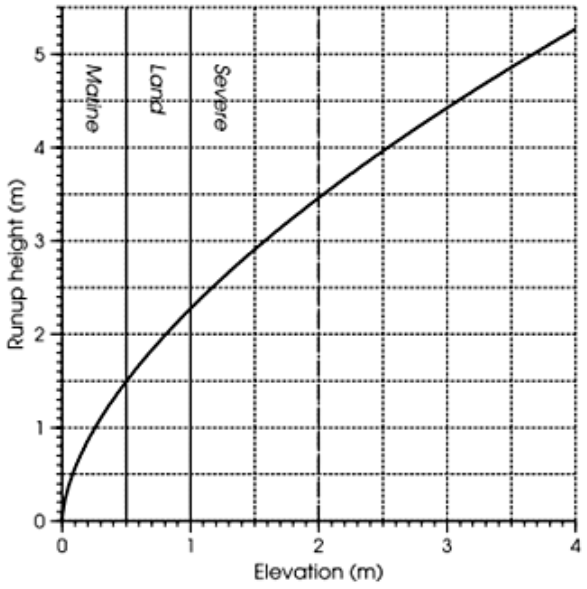

Figure 2. The Graph showing the wave elevation-run-up height relation (Synolakis 1987)

Table 1. The run-up elevation according to tsunami wave elevation (TWE) literature of the Al-Hoceima region

Author	TWE (m)	Run-up (m)
Álvarez-Gómez et al. 2011	1 m	2.5
Sørensen et al. 2012	1 m	2.5
Basquin et al. 2021	1 m	2.5

1) (Gonzalez and Medina 1998). The Spanish coast between Malaga and Adra, and the African coast between Al-Hoceima and Melilla are more exposed to the impact of tsunamis generated in the Alboran Sea (Álvarez-Gómez et al. 2011; Basquin et al. 2021; Gonzalez and Medina 1998).

Tsunamis phenomenon is a series of travelling waves of extremely long length and period, usually generated by an abrupt deformation of seafloor (Bernard and Titov 2015; Estrada et al. 2021; Meyyappan et al. 2015; Papadopoulos et al. 2014; Röbke and Vött 2017), it is characterized by three phases: the generation, the propagation and the inundation (Fajri et al. 2021; Röbke and Vött 2017). Despite the inundation phase being very important, however, there are few studies concerning with the impact of coastal flooding due to tsunami wave run-up on the coastal areas. The run-up height is the vertical distance between the ground surface and the water surface (Röbke and Vött 2017), we have to take into account that the height of the run-up, will be much higher than the elevation (Fig. 2) (Álvarez-Gómez et al. 2011). Throughout, the run-up can calculate used this equation (1) proposed by (Synolakis 1987) in the case of breaking wave:

$$R/d = 0.918 \cdot (H/d)\ 0.606 \quad (1)$$

where: R – the run-up height,
d – the depth where the elevation is obtained,
β – the slope of the bottom,
H – the value of the elevation.

This study aims at the risk mapping of coastal flooding areas due to tsunami wave run-up using a novel model which is DAS and geographic information system (GIS).

Study area

The Nekor bay is located in the Alboran Sea, which is one of the basins in the Mediterranean Sea that formed during the Neogene within a region of convergence between the African and Eurasian plates (Galindo-Zaldivar et al. 2018; Stich et al. 2020). The convergence between those tectonic plates is at a rate of 4–5 mm/yr (Estrada et al. 2021). Therefore, the Alboran Sea separates the Ibero area in Spain from the Maghreb in Morocco and the Western part of Algeria (Amir 2014). Moreover, the geomorphological and geophysical data show evidence of recent ruptures and faults large enough to generate great earthquakes (Mauffret et al. 2007). The tectonic features of the Alboran Sea are characterized by a fault system composed of short strike-slip faults and short dip-slip

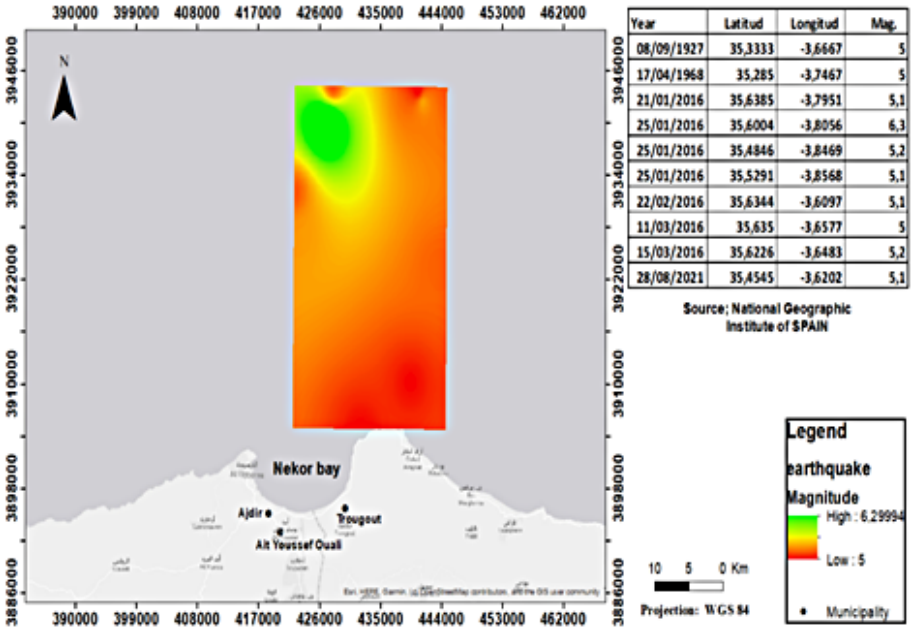

Figure 3. The distribution of earthquakes near to the Nekor bay

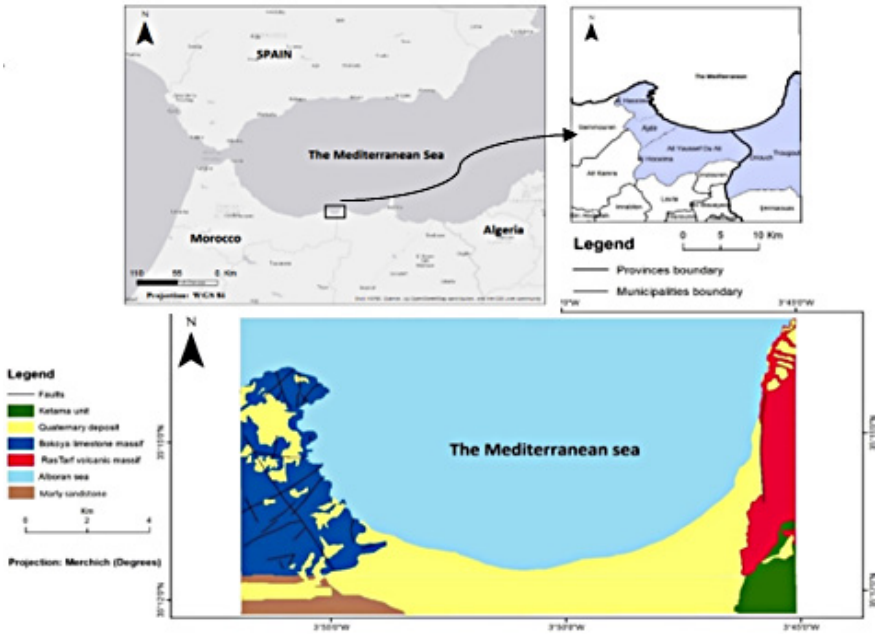

Figure 4. The simplified geological map of the study area and its administrative location

(Gonzalez and Medina 1998), the strike-slip fault is thought to be capable of generating only moderate seafloor deformation (Estrada et al. 2021), whereas the new findings suggest that the tsunamigenic potential of strike-slip faults is more important than previously thought (Estrada et al. 2021). In this context, there are several strike-slip faults continued to the proximities of the Nekor bay (Buforn et al. 2017), these faults can generate tsunami waves. According to the National Geographic Institute (IGN), 10 earthquakes, recorded in the north of Nekor bay between 1927 and 2021, have magnitude greater than 5 (Fig. 3).

The Nekor bay is situated in the east of the Al Hoceima city, Northern of Morocco between 35.25434 N and 35.26583 N latitude, 3.91526W, and 3.75733 W longitude. It has a coast length of approximately 26 kilometers (Taher at al. 2021). It is located on the southern shore of the Alboran sea and bounded to the south by the Nekor quaternary, to the east by the Ras Tarf Neogene volcanic massif, and to the west by the Bokoya limestone massif (Fig. 4). Its territory belongs to two provinces: Al-Hoceima with three municipalities: Al-Hoceima, Ajdir, Ait Youssef Ouali, and Driouch province with one municipality which is Trougout. Our study area is located in the most seismic and tectonic regions of north Africa that have witnessed several strong earthquakes (Buforn et al. 2017; Kariche et al. 2018; Stich et al. 2020), and contain many faults, especially at the west such as Ajdir fault, Boujibar fault, at the east Trougout is the main fault (Poujol et al. 2014).

MATERIALS AND METHODS

The DAS model

The current study presents a novel model to map coastal flooding potential zones in Nekor bay, which considers three important natural parameters for coastal flooding: Distance from the coastline, altitude and slope. By integrating the GIS environment and using several data sources (Google earth and digital elevation model) the inundation map was derived using equation 2. The methodology adopted in the study is shown in Figure 5.

$$CF = D * A * S \quad (2)$$

where: CF – Coastal Flooding,
D – Distance from the coastline (m),
A – Altitude (m),
S – Slope (degree).

Distance from coastline factor (D)

The coastal flooding concerns only the areas near the coast. Therefore, the distance or proximity to the coastline is an important factor. The coastal flooding risk increases the closer to the coastline, and vice versa, especially for the lower altitude areas such as plains and estuaries. The distance from the coastline map (Fig. 6) was extracted using multiple buffer tools in a GIS environment. Based on Table 2, the distance from the coastline is divided into 4 classes. the highest score was assigned to the class with the shortest distance from coastline and vice versa.

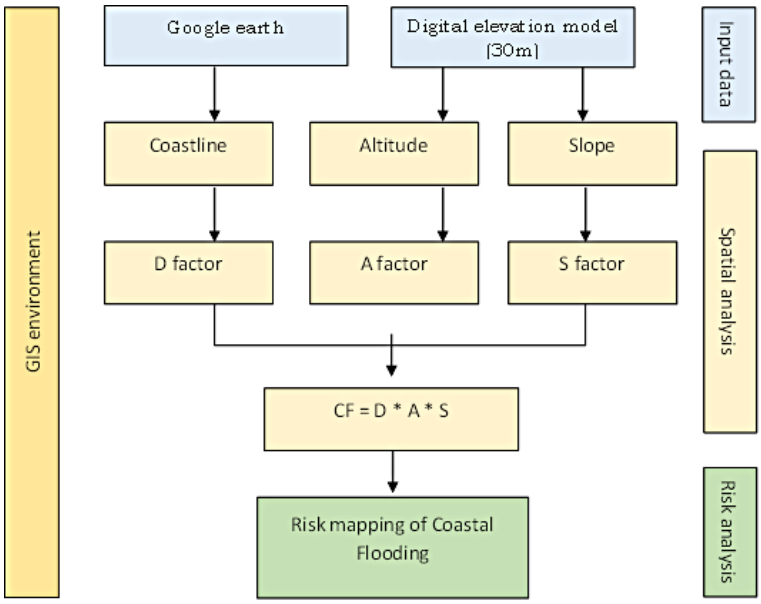

Figure 5. The flowchart of the DAS model

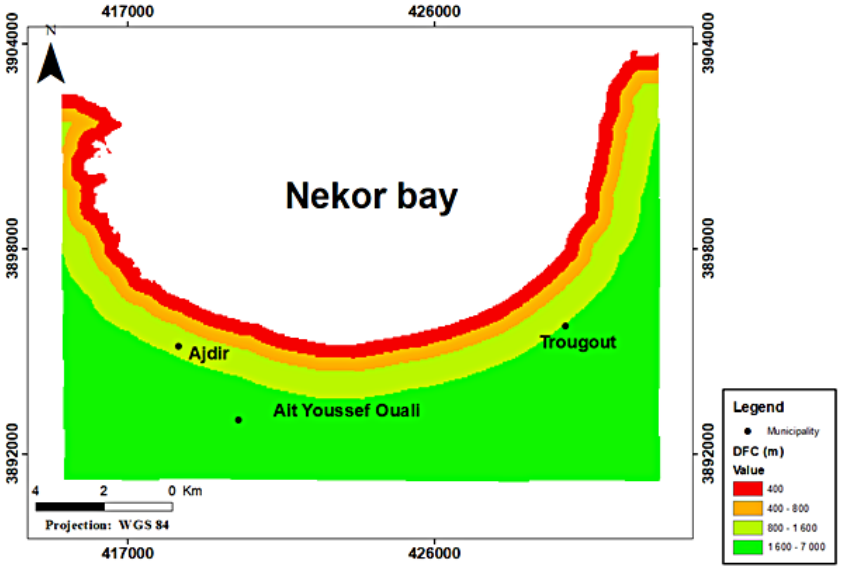

Figure 6. The distance from coastline map

Table 2. The variable distance and scoring

Altitude (m)	Indice
0–2	5
2–4	4
4–6	3
6–8	2
>8	1

Altitude factor (A)

The low-lying areas such as coastal plains could be threatened more than high areas. Therefore, the use of DEM in the GIS environment might be better in illustrating the low-lying areas along a coast that may be vulnerable to flooding (Seenath, Wilson, and Miller 2016). The Nekor bay contains Nekor plain (Fig. 7. Ph. 2) with lowers altitudes bordered by the limestone and volcanic (Fig. 7. Ph. 1 and 3) massif with the highest altitude.

The elevation map of Nekor bay was extracted from DEM (30m) downloaded from the United States Geological Survey (USGS). The results obtained show that the study area has elevations ranging from 0 to 608 m (Fig. 7). Based on Table 3, the elevation class is divided into 5 classes. the lowest score was assigned to the areas with the highest altitude and vice versa.

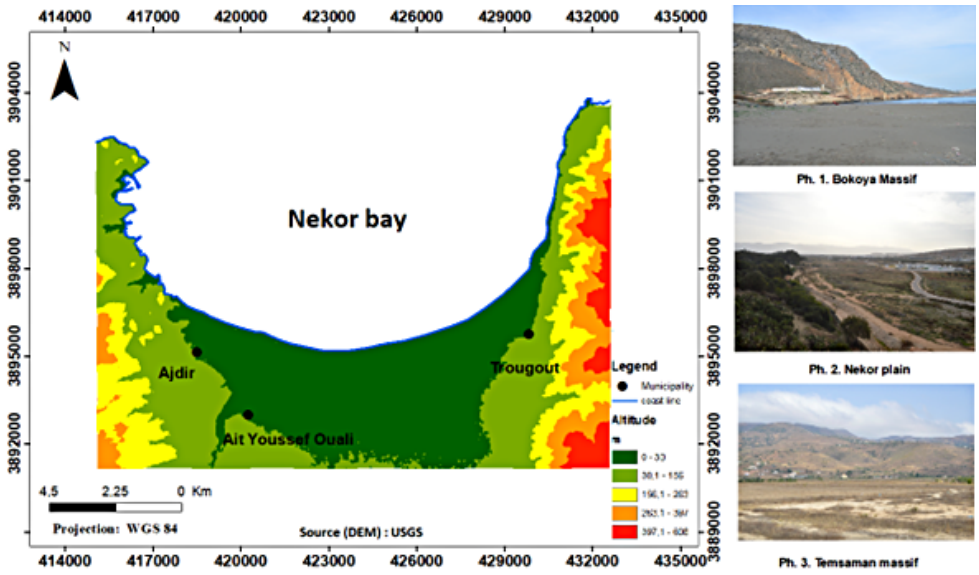

Figure 7. The altitude map of the study area

Table 3. The variable Altitude and scoring

Distance from coastal (m)	Indice
0–400	4
400–800	3
800–1200	2
>1200	1

Table 4. The variable Slope and scoring

Slope (°)	Indice
0–1	5
1–3	4
3–5	3
5–15	2
>15	1

Slope factor (S)

The flat topography of the region at low altitudes increases the risk of inundation (Omira et al. 2010). Therefore, the Nekor plain (Fig. 7. Ph. 2) is the most threatened area by coastal inundation because of its flat topography, while the limestone and volcanic massif have incline topography.

The slope map (Fig. 8) was also extracted from the same EDM mentioned above. The results obtained show that the slope rate range between 0 and 76 degrees (Fig. 8). Based on Table 4, the slope class is divided into 5 classes. The highest score was assigned to the areas with the lowest slope degree, and vice versa.

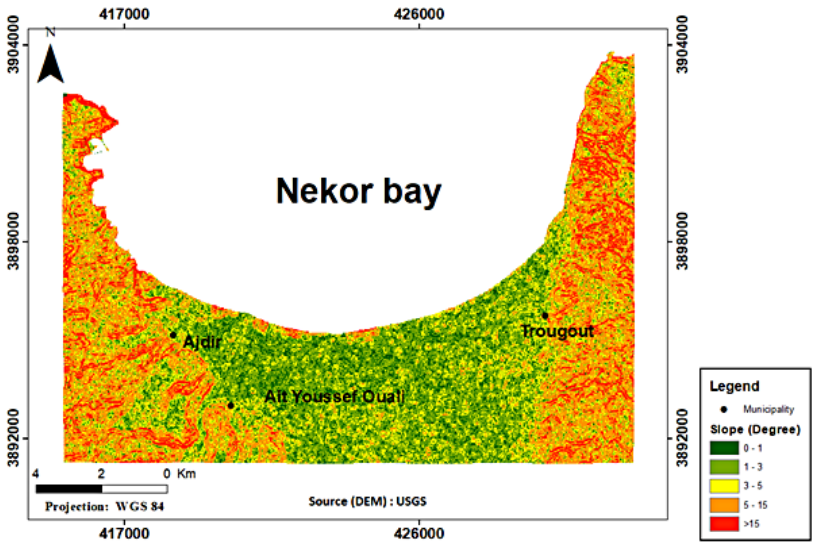

Figure 8. The slope map of the study area

The coastal flooding simulation

The validation of the DAS model needs the coastal flooding simulation. The 4 scenarios (1 m, 2 m, 3 m, 4 m) of the inundation simulation are based on the run-up elevation according to tsunami wave elevation (TWE) literature of the Al-Hoceima region (Table 2). The data (DEM and google earth) used in this study are the same used in the DAS model. The methodology adopted is shown in Figure 9. Throughout, the coastal inundation simulation concerns only the Nekor plain because of its flat topography and the low altitude, whereas the two limestone and volcanic cliffs are not concerned. Recently, the Nekor coastal plain has been experiencing rapid development and its attractiveness will continue in the future due to the recent implementation of heavy touristic projects. The Nekor plain contains two rivers that flow into the Nekor coastline at Souani beach for Ghiss river and Tayath beach for Nekor river. The Ghiss river is the limit between the two communes Ait Youssef Ouali and Ajdir, while Oued Nekor makes the limit between the two communes Ait Youssef Ouali and Trougout.

The land use map

The land use map (Fig. 10) was obtained by mapping land use classes at inside three kilometers from the coastline using buffer tools in GIS. The

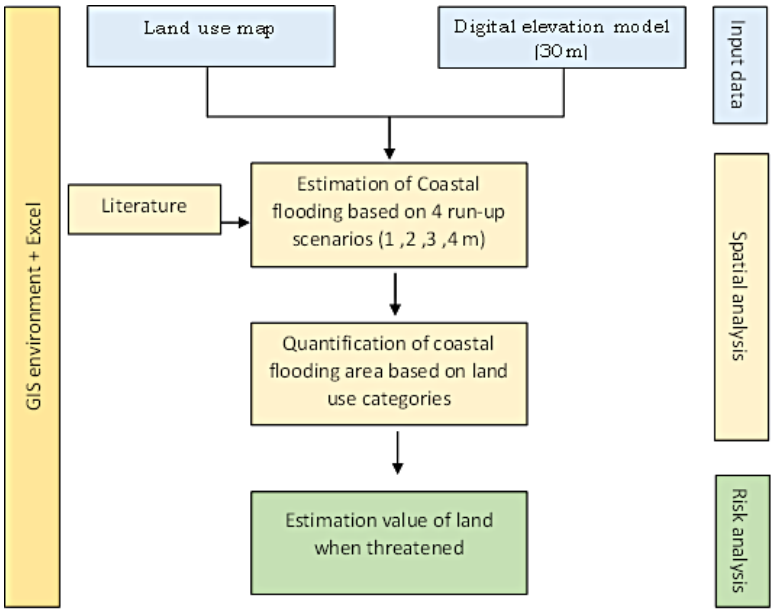

Figure 9. The flowchart of the coastal flooding simulation

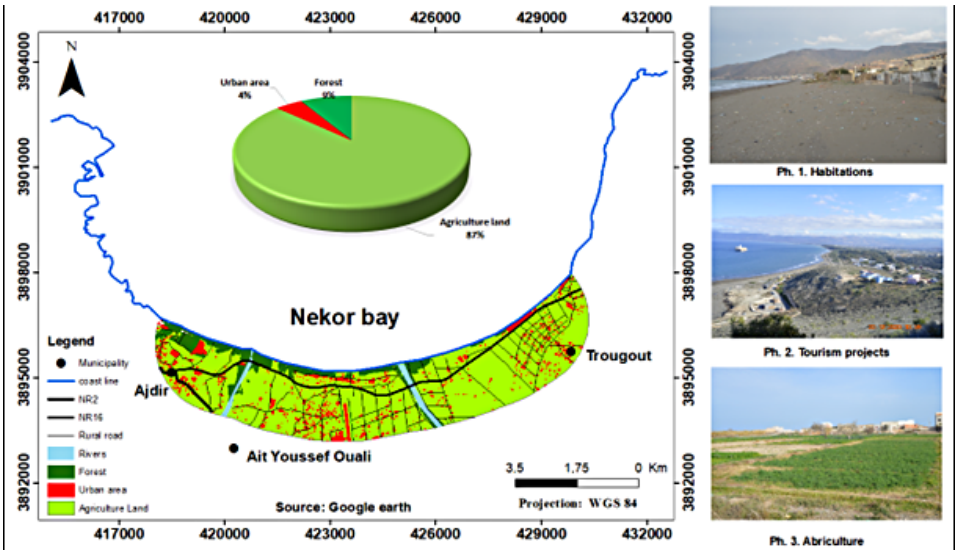

Figure 10. The land use map of the study area

Table 5. The % of land use classes

Classe	km²	%
Agriculture land	22.33024	87
Urban area	1.147082	4
Forest	2.176678	9

principal land use classes include agriculture (87%), Forest (9%), urban area (4%) (Table 5). Whereas the coastal forest in the study area has many functions and effects to reduce tsunami disaster as well as to reduce tsunami energy (Álvarez-Gómez et al. 2011; Estrada et al. 2021; Fajri et al. 2021; Szczuciński et al. 2006), and the coastal deforestation in Sfiha-Souani beaches to build touristic projects increase tsunami threat. The urban area includes habitations, schools, mosques, roads, health and social centers, wastewater treatment plant, desalination plant, airport, historical and archeological sites,…etc. The maximum population density of Ajdir, Ait youssef Ouali and Trougout municipalities are respectively 284, 333 and 101 population/km² (Fig. 11).

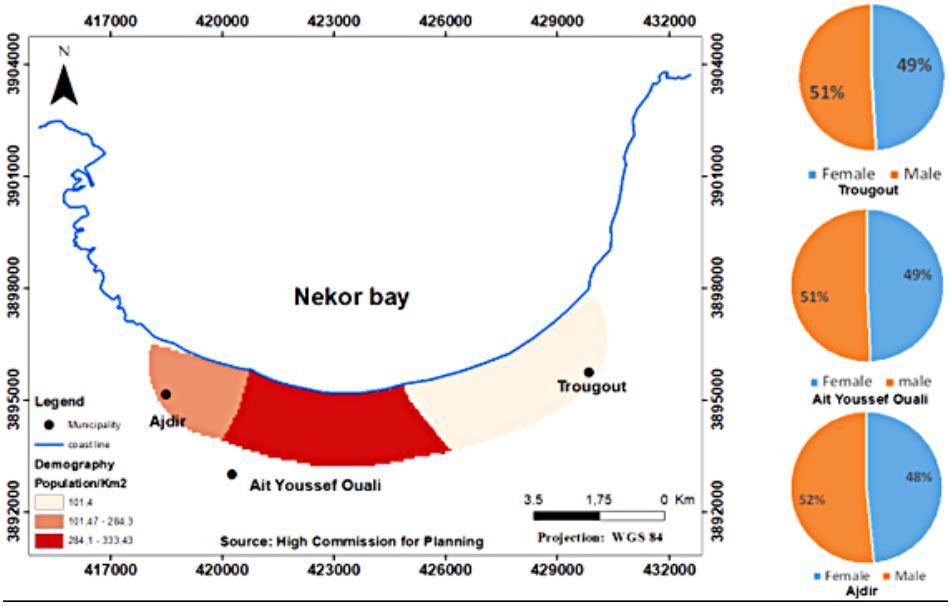

Figure 11. The population map (2014) of the study area

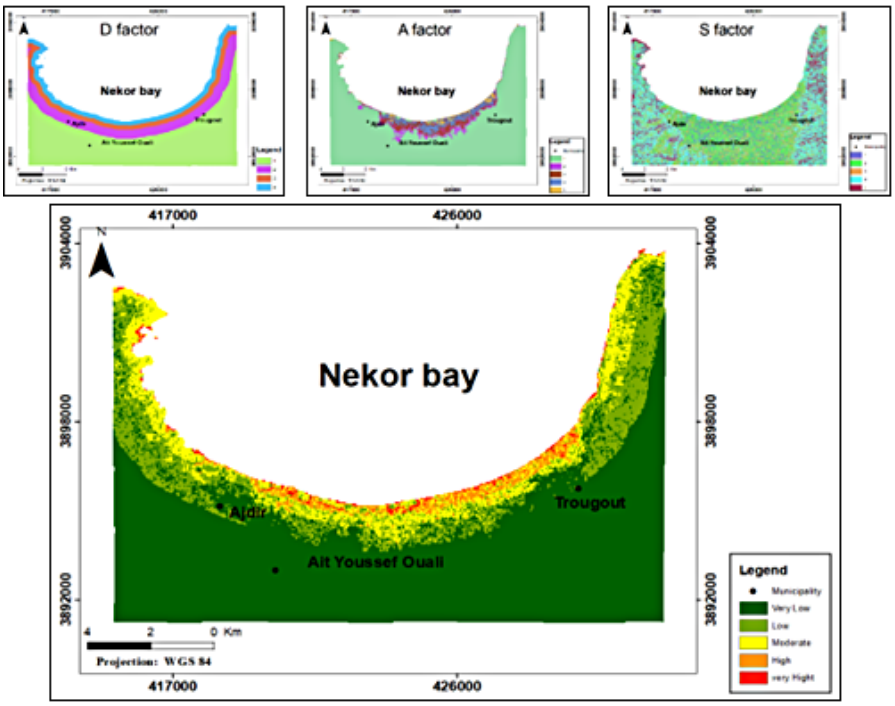

Figure 12. The risk coastal flooding map of the study area

RESULT AND DISCUSSION

In this section, we present and discuss the results for the risk mapping using a novel DAS model and the coastal flooding simulation due to tsunami wave run-up. Moreover, we present the results pertaining to scenario analysis, besides the coastal flooding maps and damage exposure estimates were calculated for each scenario. The risk coastal flooding map of the Nekor bay by integrating the DAS model is shown in Figure 12 and was obtained by integrating the distance from the coastal, the Altitude and the Slope factors in GIS using Equation (2). The inland penetration is strongly influenced by these factors, besides wave energy (Röbke and Vött 2017). In this model the wave energy was not taken into account because it depends on many factors (refraction, diffraction, speed, height, steepness… etc.). The risk mapping map was classified into 5 categories (very low, low, moderate, height and very height), and the maximum length of height risk was 1 km from the coast to the Nekor plain. Furthermore, the areas which are more exposed to the impact of tsunamis generated in the Alboran Sea are the Nekor plain, the results obtained are logical and acceptable. Nevertheless, the coastal flooding simulation is using the GIS technique needed to confirm the result obtained by the DAS model. The use of GIS for coastal flood simulation is not new. There are many other methods available to simulate coastal inundation (e.g. (Al Hatrushi S 2014; Seenath, Wilson, and Miller 2016; Ward et al. 2011)). There are two main approaches: planar models and hydrodynamic models (Ward et al. 2011). The Planar models were used in this study, use as input the run-up elevation and distribute over a DEM. The risk coastal flooding map of the study area is shown in Figure 13, the area (Fig. 14a) and the

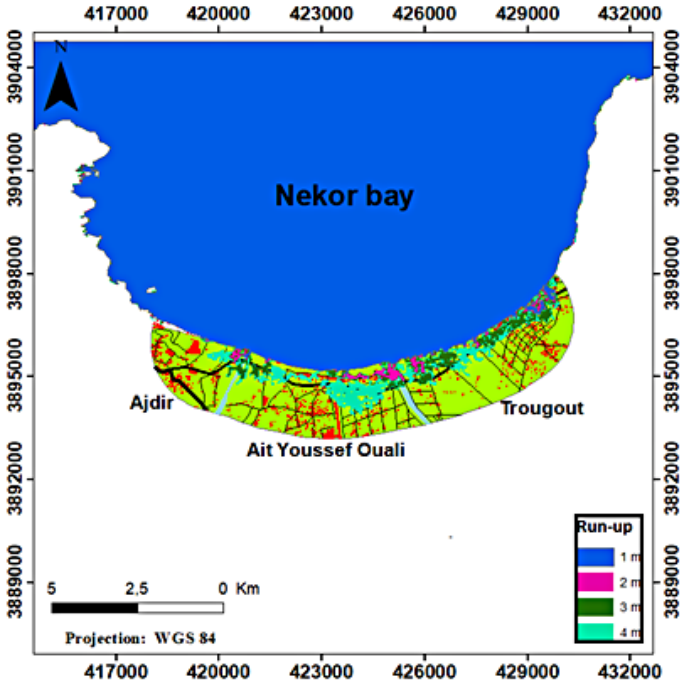

Figure 13. The risk coastal flooding map of the study area

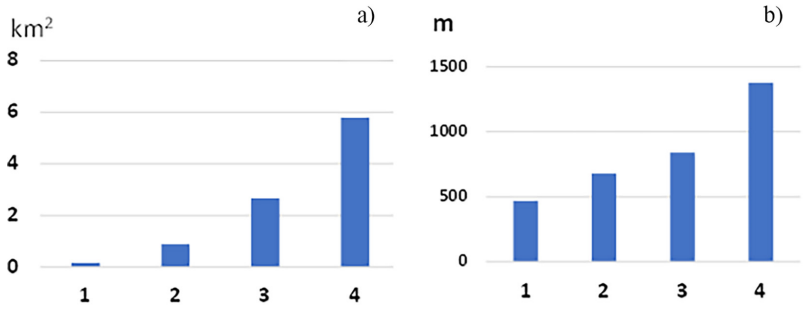

Figure 14. The coastal flooding area (a) and length (b) according to run-up elevation

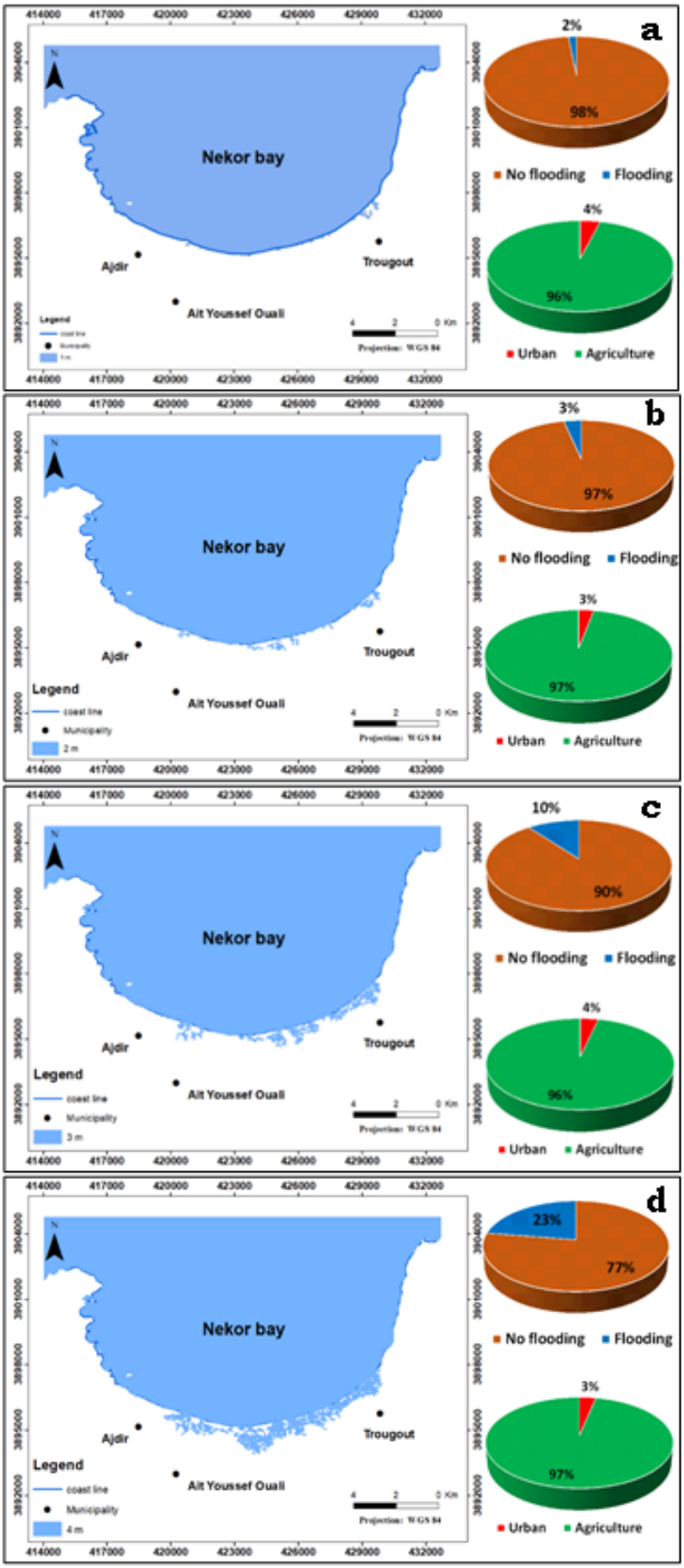

Figure 15. The 4 scenarios of coastal flooding: a = 1 m, b = 2 m, c = 3 m, d = 4 m

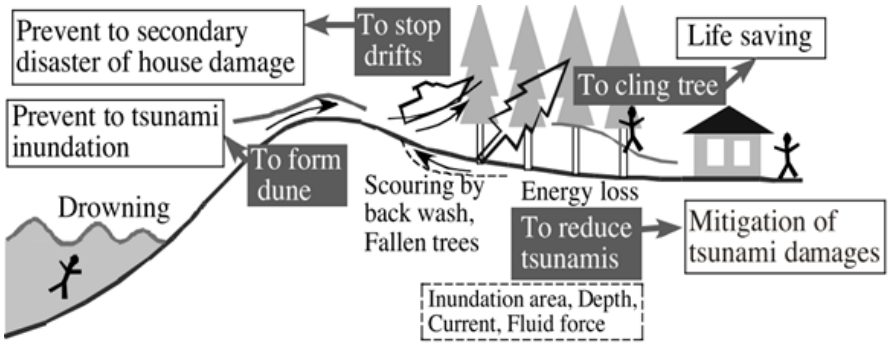

Figure 16. Functions and effects of coastal control forest to prevent tsunami disaster (Harada and Imamura 2005)

length (Fig. 14b) of the flooding increase with increasing of the run-up elevation. Therefore, the flooding area represents run-up elevation scenarios 1 m, 2 m, 3 m, and the worst scenario 4 m respectively 2%, 3%, 10%, and 23% of the study area. Furthermore, the damage estimation of urban area and agriculture was respectively 2%, 98% for run-up 1 m (Fig. 14a), 3%, 97% for run-up 2m (Fig. 15 b), 4%, 96% for run-up 3m (Fig. 15c), and for the worst scenario 4 m was 3%, 97% (Fig. 15d). Therefore, the results obtained show that the major potential impact of coastal flooding in Nekor plain is the salinization of agricultural land. The intersection between the two heights risk categories area and the 4 run-up scenarios (1, 2, 3, 4 m) are respectively 100%, 100%, 100% and 82%. Therefore, the DAS model using 3 natural parameters is useful for the risk mapping of coastal flooding, despite the neglect of other parameters such as wave energy.

According to the 4 scenarios of coastal flooding (Fig. 14), the Trougout municipality at the east of the study area is the most affected by coastal flooding, whereas the Ajdir municipality at the west is the least affected, besides the Ajdir coast is protected by densely coastal forest (Álvarez-Gómez et al. 2011; Estrada et al. 2021; Fajri et al. 2021; Szczuciński et al. 2006) counter to the Trougout coast. Furthermore, the urban area of the coastal Trougout contains 5 schools, 4 mosques, one touristic project, Hotel, beside the habitations, all this infrastructure are threatened by coastal flooding and its potential impact increase in summer with increasing population numbers (immigrants and tourists). The Ait Youssef Ouali municipality also threatened by the coastal inundation, especially in the worst scenarios (Fig. 14d), it is characterized by the agricultural activities and the height density population (Fig. 11), therefore the salinization of these agricultural lands is the major potential impact which it can lead to social problems.

Coastal areas are fragile ecosystems, it need a natural and sustainable solution. Furthermore, artificial coastal barriers are expensive, it also causes damage to the coastal environment (Harada and Imamura 2005). Therefore, one of new ways is to utilize a control forest along the coast to reduce future tsunami impacts on Nekor bay (Danielsen et al. 2005; Harada and Imamura 2005; Kathiresan and Rajendran 2005; Nandasena et al. 2008; Rubinato et al. 2020), especially at the East of the study area, the forest has many functions and effects to prevent tsunami disasters (Fig. 16), besides the use of the tsunami warning system (Bernard and Titov 2015).

CONCLUSIONS

In the current study, we have used a novel DAS model in the GIS to map the potential coastal flooding areas due to tsunami wave run-up in Nekor bay. In addition, the coastal inundation simulation scenarios for the estimation of the impacts exposure, and to compare it with the DAS model results. The comparison of the two results shows there are spatial agreements between them. Nevertheless, a perspective, the DAS model can be developed by adding other factors such as wave energy. Concerning the damage estimation of the urban area and the agriculture was respectively 2%, 98% for run-up 1 m, 3%, 97% for run-up 2 m, 4%, 96% for run-up 3 m, and for the worst scenario 4 m was 3%, 97%. The east region of the study area is the most exposing to coastal flooding. In this context, we propose a controlled forest along the coast to reduce future tsunami impacts on Nekor bay.

REFERENCES

1. Adrian, C. 2009. On the Propagation of Tsunami Waves, with Emphasis on the Tsunami of 2004. Discrete and Continuous Dynamical Systems - Series B, 12(3), 525–37.
2. Álvarez-Gómez, J.A., Aniel-Quiroga I., González M., Otero L. 2011. Tsunami Hazard at the Western Mediterranean Spanish Coast from Seismic Sources. Natural Hazards and Earth System Science, 11(1), 227–240.
3. Álvarez-Gómez, J.A. et al. 2011. Scenarios for Earthquake-Generated Tsunamis on a Complex Tectonic Area of Diffuse Deformation and Low Velocity: The Alboran Sea, Western Mediterranean. Marine Geology, 284(1–4), 55–73. http://dx.doi.org/10.1016/j.margeo.2011.03.008
4. Amarni, N. et al. 2010. Évaluation de La Vulnérabilité Côtière Du Littoral Centre Ouest Algérien (Cherchell), Sous l'Angle de La Géomatique.
5. Amir, L.A. 2014. Tsunami hazard assessment in the alboran sea for the Western coast of Algeria. Journal of Shipping and Ocean Engineering, 4(April), 43–51.
6. Basquin, E., Mercier, D., Creach, A. 2021. Diagnostic Préliminaire de l'Exposition Du Littoral Méditerranéen Du Maroc Face Au Risque de Tsunami, (Jan.).
7. Becu, N. et al. 2017. Participatory simulation to foster social learning on coastal flooding prevention. Environmental Modelling and Software, 98, 1–11.
8. Bernard, E., Titov V. 2015. Evolution of tsunami warning systems and products. Philosophical Transactions of the Royal Society A: Mathematical, Physical and Engineering Sciences, 373(2053).
9. Bilskie, M.V., Hagen, S.C., Medeiros, S.C., Passeri, D.L. 2014. Dynamics of Sea Level Rise and Coastal Flooding on a Changing Landscape. Geophysical Research Letters, 41(3), 927–934.
10. Buforn, E. et al. 2017. The 2016 South Alboran Earthquake (Mw = 6.4): A Reactivation of the Ibero-Maghrebian Region? Tectonophysics, 712–713, 704–715.
11. Cazenave, A., Le Cozannet G. 2014. Sea Level Rise and Its Coastal Impacts. Earth's Future, 2(2), 15–34.
12. Danielsen, F. et al. 2005. The Asian Tsunami: A Protective Role for Coastal Vegetation. Science, 310(5748), 643.
13. Estrada, F. et al. 2021. Tsunami Generation Potential of a Strike-Slip Fault Tip in the Westernmost Mediterranean. Scientific Reports, 11(1), 1–9. https://doi.org/10.1038/s41598-021-95729-6.
14. Fajri, Z. et al. 2021. Numerical simulation of tsunami hazards in south atlantic coast: case of the city of Agadir-Morocco: preliminary result. International Archives of the Photogrammetry, Remote Sensing and Spatial Information Sciences - ISPRS Archives 46(4/W5-2021): 219–223.
15. Galindo-Zaldivar, J. et al. 2018. Imaging the growth of recent faults: The case of 2016–2017 seismic sequence sea bottom deformation in the Alboran Sea (Western Mediterranean). Tectonics, 37(8), 2513–2530.
16. Ghazali, N.H.M., Awang, N.A., Mahmud, M., Mokhtar, A. 2018. Impact of sea level rise and tsunami on coastal areas of North-West Peninsular Malaysia. Irrigation and Drainage, 67(May), 119–129.
17. Gonzalez, M., Medina R. 1998. Probabilistic Model for Tsunami-Wave Elevation along the Alboran Seacoast. Proceedings of the Coastal Engineering Conference, 2, 1168–1181.
18. Harada, K., Imamura, F. 2005. Effects of coastal forest on tsunami hazard mitigation – A preliminary investigation. Advances in Natural and Technological Hazards Research, 23(Jan.), 279–292.
19. Al Hatrushi S., Al-Buloshi A. 2014. GIS-Based Framework for the Simulation of the Impacts of Sea Level Rise and Coastal Flooding on Oman. Journal of Earth Science & Climatic Change, 5(10).
20. Hauer, M.E. et al. 2021. Assessing Population Exposure to Coastal Flooding Due to Sea Level Rise. Nature Communications, 12(1), 1–9.
21. Jevrejeva, S. et al. 2016. Coastal Sea Level Rise with Warming above 2 °C. Proceedings of the National Academy of Sciences of the United States of America, 113(47), 13342–13347.
22. Kariche, J. et al. 2018. The Al Hoceima earthquake sequence of 1994, 2004 and 2016: Stress transfer and poroelasticity in the Rif and Alboran Sea Region. Geophysical Journal International, 212(1), 42–53.
23. Kathiresan, K., Rajendran N. 2005. Coastal Mangrove Forests Mitigated Tsunami. Estuarine, Coastal and Shelf Science, 65(3), 601–606.
24. Leatherman, S.P., Zhang K., Douglas B.C. 2000. Sea Level Rise Shown to Drive Coastal Erosion. Eos, 81(6), 55–57.
25. Løvholt, F. et al. 2012. Tsunami Hazard and Exposure on the Global Scale. Earth-Science Reviews, 110(1–4), 58–73. http://dx.doi.org/10.1016/j.earscirev.2011.10.002.
26. Mauffret, A., Ammar A., Gorini C., Jabour H. 2007. The Alboran Sea (Western Mediterranean) revisited with a view from the Moroccan Margin. Terra Nova, 19(3), 195–203.
27. Meyyappan, P.L. et al. 2015. Tsunami Wave Impact on Structures. International Journal of Applied Engineering Research, 10(50), 1135–1139.
28. El Moussaoui, S. et al. 2017. Tsunami Hazard and Buildings Vulnerability along the Northern Atlantic Coast of Morocco – the 1755-like Tsunami in Asilah Test-Site. Geoenvironmental Disasters, 4(1).
29. Nandasena, N.A.K., Tanaka N., Tanimoto K. 2008. Tsunami Current Inundation of Ground With Coastal Vegetation Effects: An Initial Step Towards a Natural Solution for Tsunami Amelioration. Journal of

Earthquake and Tsunami, 2(2), 157–171.

30. Natarajan, L. et al. 2021. Flood susceptibility analysis in chennai corporation using frequency ratio model. Journal of the Indian Society of Remote Sensing, 49(7), 1533–1543. https://doi.org/10.1007/s12524-021-01331-8.
31. Nicholls, R.J., Cazenave, A. 2010. Sea-Level Rise and Its Impact on Coastal Zones. Science, 328(5985), 1517–1520.
32. Omira, R. et al. 2010. Tsunami vulnerability assessment of Casablanca-Morocco using numerical modelling and GIS tools. Natural Hazards, 54(1), 75–95.
33. Papadopoulos, G.A. et al. 2014. Historical and pre-historical tsunamis in the mediterranean and its connected seas: Geological signatures, generation mechanisms and coastal impacts. Marine Geology, 354, 81–109. http://dx.doi.org/10.1016/j.margeo.2014.04.014.
34. Papathoma, M., Dominey-Howes D. 2003. Tsunami Vulnerability Assessment and Its Implications for Coastal Hazard Analysis and Disaster Management Planning, Gulf of Corinth, Greece. Natural Hazards and Earth System Science, 3(6), 733–747.
35. Papathoma, M., Dominey-Howes D., Zong Y., Smith D. 2003. Assessing Tsunami Vulnerability, an Example from Herakleio, Crete. Natural Hazards and Earth System Science, 3(5), 377–389.
36. Pethick, J. 2001. Coastal Management and Sea-Level Rise. Catena, 42(2–4), 307–322.
37. Poujol, A. et al. 2014. Active Tectonics of the Northern Rif (Morocco) from Geomorphic and Geochronological Data. Journal of Geodynamics, 77, 70–88. http://dx.doi.org/10.1016/j.jog.2014.01.004
38. Qu, Y., Jevrejeva, S., Jackson, L.P., Moore, J.C. 2019. Coastal Sea Level Rise around the China Seas. Global and Planetary Change, 172, 454–463. https://doi.org/10.1016/j.gloplacha.2018.11.005
39. Röbke, B.R., Vött, A. 2017. The tsunami phenomenon. Progress in Oceanography, 159(Sept.), 296–322. http://dx.doi.org/10.1016/j.pocean.2017.09.003.
40. Rubinato, M., Heyworth, J., Hart, J.. 2020. Protecting Coastlines from Flooding in a Changing Climate: A Preliminary Experimental Study to Investigate a Sustainable Approach. Water (Switzerland), 12(9).
41. Samaras, A.G., Karambas, T.V. 2021. Modelling the Impact of Climate Change on Coastal Flooding: Implications for Coastal Structures Design. Journal of Marine Science and Engineering, 9(9).
42. Seenath, A., Wilson, M., Miller, K. 2016. Hydrodynamic versus GIS Modelling for Coastal Flood Vulnerability Assessment: Which Is Better for Guiding Coastal Management? Ocean and Coastal Management, 120, 99–109. http://dx.doi.org/10.1016/j.ocecoaman.2015.11.019
43. Smith, J.M.K., Cialone, M.A., Wamsley, T.V., McAlpin, T.O. 2010. Potential Impact of Sea Level Rise on Coastal Surges in Southeast Louisiana. Ocean Engineering, 37(1), 37–47. http://dx.doi.org/10.1016/j.oceaneng.2009.07.008
44. Sørensen, M.B. et al. 2012. Probabilistic Tsunami Hazard in the Mediterranean Sea. Journal of Geophysical Research: Solid Earth, 117(1), 1–15.
45. Stich, D. et al. 2020. Slip Partitioning in the 2016 Alboran Sea Earthquake Sequence (Western Mediterranean). Frontiers in Earth Science, 8(Sept.), 1–19.
46. Syamsidik, et al. 2019. Post-Tsunami Survey of the 28 September 2018 Tsunami near Palu Bay in Central Sulawesi, Indonesia: Impacts and Challenges to Coastal Communities. International Journal of Disaster Risk Reduction, 38(March), 101229. https://doi.org/10.1016/j.ijdrr.2019.101229
47. Synolakis, C.E. 1987. The Runup of Solitary Waves. Journal of Fluid Mechanics, 185(May), 523–545.
48. Szczuciński, W. et al. 2006. Environmental and Geological Impacts of the 26 December 2004 Tsunami in Coastal Zone of Thailand - Overview of Short and Long-Term Effects. Polish Journal of Environmental Studies, 15(5), 793–810.
49. El Talibi, H. et al. 2016. New Sedimentary and Geomorphic Evidence of Tsunami Flooding Related to an Older Events along the Tangier-Asilah Coastal Plain, Morocco. Geoenvironmental Disasters, 3(1). http://dx.doi.org/10.1186/s40677-016-0049-6
50. Vargas, G. et al. 2011. Coastal uplift and tsunami effects associated to the 2010 Mw8.8 Maule earthquake in Central Chile. Andean Geology, 38(1), 219–238.
51. Wang Y. and Marsooli R. 2021. Dynamic modeling of sea-level rise impact on coastal flood hazard and vulnerability in New York City's built environment. Coastal Engineering, 169(Aug.), 103980. https://doi.org/10.1016/j.coastaleng.2021.103980.
52. Ward, P.J. et al. 2011. Coastal Inundation and Damage Exposure Estimation: A Case Study for Jakarta. Natural Hazards, 56(3), 899–916.
53. Werner, A.D., Simmons, C.T. 2009. Impact of Sea-Level Rise on Sea Water Intrusion in Coastal Aquifers. Ground Water, 47(2), 197–204.
54. White, N.J., Church J.A., Gregory J.M. 2005. Coastal and global averaged sea level rise for 1950 to 2000. Geophysical Research Letters, 32(1), 1–4.
55. Xie, P., Chu V.H. 2020. The Impact of Tsunami Wave Force on Elevated Coastal Structures. Coastal Engineering, 162(Sept.), 103777. https://doi.org/10.1016/j.coastaleng.2020.103777
56. Yalciner, A.C. et al. 2011. Field Survey on the Coastal Impacts of March 11, 2011 Great East Japan Tsunami. Seismic Protection of Cultural Heritage - The World Council of Civil Engineers (WCCE), the European Council of Civil Engineers (ECCE) and the Turkish Chamber of Civil Engineers (TCCE) Joint Conference 2011, 123–40.